

First-principles investigation of ^{67}Zn isomer shifts in ZnF_2 and the chalcogenides ZnO , ZnS , ZnSe , and ZnTe

D. W. Mitchell and T. P. Das

Department of Physics, State University of New York at Albany, Albany, New York, 12222

W. Potzel, G. M. Kalvius, H. Karzel, W. Schiessl, M. Steiner, and M. Köfferlein
Physik Department E15, Technische Universität München, D-85747 Garching, Germany

(Received 28 June 1993)

All-electron, self-consistent, Hartree-Fock cluster calculations have been carried out to derive electron densities at the zinc nucleus in the series of compounds ZnF_2 (rutile-type structure), ZnO (rocksalt structure), ZnO (wurtzite structure), and the compounds ZnS , ZnSe , and ZnTe (all with the sphalerite structure). The derived density differences show a very good linear correlation with the experimental isomer shifts. The isomer shifts and results for the densities at the zinc nucleus have been combined to calculate a value for the change of the mean-square nuclear charge radius for the Mössbauer transition in ^{67}Zn of $\Delta\langle r^2 \rangle = +(13.9 \pm 1.4) \times 10^{-3} \text{ fm}^2$. Our calculations clearly show the importance of the covalency of the Zn-ligand bond for the origin of the isomer shift and fully corroborate the experimental linear correlation between decreasing isomer shift values and increasing electronegativity of the ligands. The most important contribution to the electron-density differences at the zinc nucleus comes from the Zn(4s) electrons with a smaller but significant contribution from the Zn(3s) electrons appearing to arise primarily from the repulsive influence of the ligand-ion orbitals.

I. INTRODUCTION

The 93.3 keV Mössbauer transition of ^{67}Zn is a solid-state probe with extremely high resolution for the determination of small changes in γ -ray energy,¹⁻³ a consequence of the relatively long half-life of 9.1 μs for the first excited state resulting in a minimal observable width of only 0.31 $\mu\text{m/s}$. Not surprisingly, ^{67}Zn Mössbauer spectroscopy has been the subject of diverse experimental investigations^{4,5} including hyperfine properties,⁶⁻¹² lattice dynamics,^{8,9} phase transitions,^{10,11} and the gravitational red shift.¹³ Due to the narrow linewidth of this resonance, isomer shifts are prominent spectral features and are measurable with high precision.^{6,7} Mössbauer isomer shifts are now available⁶⁻¹² for a very wide range of zinc compounds ranging from the ionic insulator ZnF_2 to the broadband semiconductor ZnTe to metallic alloys. Our goal is the comprehensive theoretical investigation of ^{67}Zn isomer shifts in a wide range of binary ionic Zn compounds. This is a computationally difficult problem since differences in electron contact density (defined here as the total electron density at the zinc nucleus) are very small in comparison to the contact densities of the individual systems and also because Zn only has one preferred ionic state, namely Zn^{2+} , the small density differences resulting primarily from subtle changes in the Zn-ligand chemical bond. A major motivation of this work is to explain quantitatively the trend in the observed isomer shifts in going over a series of related compounds for which ^{67}Zn isomer shift data are available. Electron charge densities at the ^{67}Zn nucleus are calculated here by the Hartree-Fock (HF) cluster procedure¹⁴⁻²² for the series of binary compounds ZnF_2 with the tetragonal ru-

tile structure,²³ and the chalcogenides, ZnO in both the rocksalt²⁴ and wurtzite²⁵ structures, and ZnS , ZnSe , and ZnTe all with the cubic sphalerite.^{26,27} The lattice parameters, coordinations, and nearest-neighbor distances for these systems are summarized in Table I. The calculated electron densities are used to quantitatively interpret the observed trends in the isomer shifts in terms of the chemical bonding and electronic structures in these systems. Also, the calculated densities are combined with experimental isomer shifts to evaluate the nuclear param-

TABLE I. Crystal structures and lattice parameters of zinc compounds studied.

System	Crystal structure	Lattice parameters	Zn-X (Å)
ZnF_2	Tetragonal (rutile) ^a	$a = 4.705 \text{ \AA}$	2(F) 2.012
		$c = 3.134 \text{ \AA}$	4(F) 2.045
		$x = 0.3024$	
ZnO	Cubic (rocksalt) ^b	$a = 4.280 \text{ \AA}$	6(O) 2.14
ZnO	Hexagonal (wurtzite) ^c	$a = 3.2499 \text{ \AA}$	1(O) 1.9915
		$c = 5.2066 \text{ \AA}$	3(O) 1.9735
		$u = 0.3825$	
ZnS	Cubic (sphalerite) ^c	$a = 5.406 \text{ \AA}$	4(S) 2.3409
ZnSe	Cubic (sphalerite) ^d	$a = 5.65 \text{ \AA}$	4(Se) 2.447
ZnTe	Cubic (sphalerite) ^d	$a = 6.07 \text{ \AA}$	4(Te) 2.628

^aReference 23.

^bReference 24.

^cReference 25.

^dReference 26.

^eReference 27.

eter $\Delta\langle r^2 \rangle$, the difference in mean-square nuclear charge radii between the excited (Mössbauer) and ground nuclear states.

The Mössbauer isomer shift²⁸ is a unique experimental result which can provide atomic scale chemical structure information in solid-state systems observed as changes in the isotropic density at the Mössbauer nucleus. Along with the nuclear-quadrupole interaction²⁹ which is dependent on the anisotropy of the charge density, isomer shifts provide a valuable opportunity to make a comprehensive test of the calculated electron densities at nuclear sites. The isomer shift (S) between two different systems is given by the relation;³⁰

$$S = \alpha \Delta |\psi(0)|^2, \quad (1)$$

where $\Delta |\psi(0)|^2$ is the difference in the electron density at the nucleus in the two systems with α known as the isomer-shift calibration constant³⁰ which contains all of the nuclear information. This density difference should ideally be calculated using a fully relativistic method, a rather difficult task. However, it has been shown from a number of investigations that it is a satisfactory approximation to use a nonrelativistic result scales by a constant factor $S'(Z)$ (with Z representing the atomic number of the nucleus), the ratio of the densities at the nuclei in atomic systems from relativistic Dirac-Fock and nonrelativistic Hartree-Fock calculations, this factor^{31,32} being 1.40 for zinc. For our purposes then, the Hartree-Fock density difference $\Delta\rho(0)$ at the zinc nucleus for the two systems has to be calculated and $\Delta |\psi(0)|^2$ is approximated as $S'(Z)\Delta\rho(0)$. Hereafter, we employ the notational convention that $\rho(0)$ refers to nonrelativistic Hartree-Fock contact density, while $|\psi(0)|^2$ refers to relativistic contact density. Equation (1) can be alternatively written as³⁰

$$S = \beta \Delta\langle r^2 \rangle S'(Z) \Delta\rho(0), \quad (2)$$

where $\Delta\langle r^2 \rangle$ is the difference in the mean-square radii of the nucleus in the first excited Mössbauer and ground states, with³¹ $\beta = 1.95 \times 10^3 \text{ fm}^{-2} a_0^3 \mu\text{m/s}$ for the 93.3 keV transition of ^{67}Zn and the charge-density difference between absorber and source $\Delta\rho(0)$ obtained from nonrelativistic calculations with $S'(Z) = 1.40$. In Eq. (2), $\Delta\langle r^2 \rangle$ is measured in units of fm^2 , $\Delta\rho(0)$ is in atomic units a_0^{-3} , and S is in $\mu\text{m/s}$. A value of $\Delta\langle r^2 \rangle$ has been obtained recently³³ to be $+(17.8 \pm 3.9) \times 10^{-3} \text{ fm}^2$ from a combination of the experimental isomer shift between zinc metal and ZnO (wurtzite) and the change in electron capture decay constant in the same systems for ^{65}Zn . Thus, there are two major challenges to theory. These are, first, to quantitatively explain the trend in the observed isomer shifts as one goes through the series of compounds investigated and second, to derive $\Delta\langle r^2 \rangle$ and compare with the experimentally determined³³ result. The present work is addressed at these two challenges.

Section II gives a description of the procedure used for the electronic structure and the approximations involved. Section III contains the results and discussion. Included here are the calculated individual molecular-orbital contributions to $\rho(0)$, a discussion of the origin of the core

and valence contributions, our results for the valence electronic structures, and a derivation of $\Delta\langle r^2 \rangle$ with comparison to experiment, and other calculations. Section IV presents a few concluding remarks.

II. PROCEDURE

The all-electron self-consistent Hartree-Fock cluster procedure^{14,22} has been used recently with success for the investigation of nuclear-quadrupole interactions¹⁹⁻²¹ in a number of ionic crystals and high- T_c systems,²² and for the study of magnetic hyperfine interactions^{19,22} as well. Also, this method has been successfully applied¹⁵ to the calibration of the isomer shift for ^{57}Fe . The Hartree-Fock cluster procedure, however, has not been applied to the study of ^{67}Zn isomer shifts before, nor to such a wide range of ionic compounds as is carried out here.

In this method, which utilizes the Hartree-Fock-Roothaan variational approach,³⁴ the solid-state system is simulated¹⁶ by a finite number of ions, with the ion whose properties are being studied, in this case the zinc ion, at the center. The number of ions chosen in such calculations is based on a compromise between accuracy and practicability. The influence of the rest of the lattice is incorporated by including in the Hartree-Fock potential for the electrons in the cluster, the potential due to the ions outside the cluster, considering their influence to be described as those due to point charges. In particular, the cluster is surrounded by spherical shells of point charges located at lattice sites out to about 10 to 12 Å from the central atom with the charges on the outermost shells adjusted²⁰ to give the correct Madelung potential at all the nuclei within the cluster and also to give charge neutrality for the entire system of cluster plus external point charges. The incorporation of this potential due to the rest of the lattice not only allows us to essentially include the whole crystal in our calculations but also provides the important stabilization potential necessary to localize the electron distribution in diffuse negative ions like O^{2-} .

For our calculations, clusters $(\text{ZnX}_4)^{6-}$ involving zinc and its nearest-neighbor ligands with $X = \text{O}, \text{S}, \text{Se},$ and Te are utilized for ZnO (wurtzite), ZnS, ZnSe, and ZnTe. For ZnO (rocksalt) and tetragonal ZnF_2 , the chosen clusters are $(\text{ZnO}_6)^{10-}$ and $(\text{ZnF}_6)^{4-}$, respectively. Contracted Gaussian-type functions³⁵⁻³⁷ are employed in these variational Hartree-Fock calculations. The chosen basis sets are extensive, of double-zeta-plus polarization quality.³⁷ For zinc, Wachters' full double-zeta basis set,³⁸ augmented with a diffuse p exponent³⁹ (exponent 0.3) is used to give a better description of the $\text{Zn}(4p)$ electrons. While empty for the free atom, the $\text{Zn}(4p)$ orbitals may be important for bonding in solids. The contraction scheme of this basis set in the terminology³⁶ that is commonly used for quantum chemical calculations, is $\text{Zn}(8s6p2d):(62111111/511111/41)$. The use of a zinc basis set optimized for the neutral atom is not unreasonable since Zn^{2+} essentially represents the core states of the neutral atom and basis sets involved in expanding their wave functions should not be too different from that for the neutral atom. For the ligands, we have also em-

ployed basis sets optimized for the neutral atom, but with several considerations in their choice. For fluorine, a basis set which has been optimized for the free F^{1-} anion is also used. The fluorine basis sets optimized for neutral and ionic fluorine are referred to here as, respectively, the F^0 basis set and the F^{1-} basis set. Comparison of the calculated results using these two basis sets allows an estimate of the confidence in the use of the other basis sets since it is not entirely clear whether basis sets optimized for neutral atoms are sufficient in these systems. However, since Hartree-Fock calculations are variational, a sufficiently flexible basis set in the variational sense should give similar results for properties whether that basis set originated from atomic calculations on free atoms or free ions. Our earlier experience²¹ regarding the ^{67}Zn nuclear-quadrupole interaction in ZnO demonstrated that both basis sets optimized for the neutral oxygen atom and basis sets optimized for O^{2-} confined in a Watson sphere potential gave similar results for calculated electric-field gradients. In all of the basis sets used in the present work, the most diffuse exponents have been uncontracted from the rest of the basis set for greatest variational flexibility since these diffuse exponents are more closely associated with the valence shells of ions, which undergo the greatest change in going from free atoms to ions in solids.

Further, all of the ligand basis sets are augmented with d exponents (polarization functions)³⁶ which have two effects. First of all, polarization functions allow the ligand outer valence p shell to distort from spherical symmetry and secondly, they allow for electron occupation in the ligand valence d shell, which is empty for the neutral atoms or anions. This last point is most important for ZnS, ZnSe, and ZnTe which can be easily understood from atomic energy considerations by the following argument. The valence electronic configurations of F^{1-} , O^{2-} , and S^{2-} are, respectively, $2s^22p^6$, $2s^22p^6$, and $3s^23p^6$.

For F^{1-} or O^{2-} , the energy difference between the $2p$ and $3d$ orbitals is quite large but it is substantially smaller between $3p$ and $3d$ in S^{2-} , or $4p$ and $4d$ in Se^{2-} , or $5p$ and $5d$ in Te^{2-} . Therefore, a basis set which can include the valence d states in S, Se, and Te is important for an accurate description of chemical bonding in ZnS, ZnSe, and ZnTe. It turns out that the valence molecular orbitals responsible for $\rho(0)$ in these systems have some ligand valence d character as well.

The basis sets optimized for neutral F, O, and S are taken from Dunning³⁵ with contraction schemes $\text{F}^0(4s2p1d):(6111/41/1)$, $\text{O}(4s2p1d):(6111/41/1)$, and $\text{S}(6s4p1d):(531111/4211/1)$. For Se, Te, and F^{1-} the basis sets are taken from Huzinaga³⁶ with contraction schemes of $\text{Se}(6s5p3d):(431111/41111/211)$, $\text{Te}(7s6p4d):(4321111/421111/4111)$, and $\text{F}^{1-}(4s2p1d):(41111/31/1)$. The exponents of the single Gaussian d -polarization functions, also from Huzinaga,³⁶ are 1.29, 1.15, 0.42, 0.34, and 0.24 for, respectively, F, O, S, Se, and Te. These basis sets are of double-zeta-plus polarization quality and are considered reliable^{37,39} at the Hartree-Fock level of theory.

As a quantitative test of the use of Hartree-Fock calculations with Gaussian basis sets for calculating small changes in the electron density at the zinc nucleus, we have made a comparison of $\Delta\rho(0)$ obtained using Gaussian basis sets with numerical Dirac-Fock calculations⁴⁰ for different atomic configurations of zinc. Such a comparison is especially important for the Zn(s)-core electrons, since in this case a small change in the atomic orbital can give relatively large changes in the electron contact density. Table II gives results from previously published⁴⁰ fully relativistic atomic Dirac-Fock calculations and our own nonrelativistic Hartree-Fock calculations for the zinc atom in three different configurations, $\text{Zn}^{2+}(3d^{10})$, $\text{Zn}^{1+}(3d^{10}4s^1)$, and $\text{Zn}^0(3d^{10}4s^2)$. The first case, Zn^{2+} , corresponds to complete ionicity while Zn^{1+}

TABLE II. Electron contact densities for different charge states of Zn. (a) Numerical atomic Dirac-Fock calculations (Ref. 40). (b) Gaussian basis set atomic Hartree-Fock calculations with $S'(Z)=1.40$. The density differences are calculated with respect to the Zn^{2+} density. All results are in atomic units (a_0^{-3}).

	Dirac-Fock $ \psi(0) ^2(a_0^{-3})$		$\Delta \psi(0) ^2$		
	$\text{Zn}^{2+}(4s^0)$	$\text{Zn}^{1+}(4s^1)$	$\text{Zn}^0(4s^2)$	$\text{Zn}^{1+}(4s^1)$	$\text{Zn}^0(4s^2)$
1s	22 484.80	22 484.68	22 484.61	-0.12	-0.19
2s	2 231.86	2 232.04	2 232.14	+0.18	+0.28
3s	319.13	319.98	320.53	+0.85	+1.40
4s	0.00	8.62	13.16	+8.62	+13.16
$p_{1/2}$	18.99	18.99	18.99		
Total	25 054.78	25 064.31	25 069.43	+9.53	+14.65

	Hartree-Fock $\rho(0)(a_0^{-3})$		$S'(Z)\Delta\rho(0)$		
	$\text{Zn}^{2+}(4s^0)$	$\text{Zn}^{1+}(4s^1)$	$\text{Zn}^0(4s^2)$	$\text{Zn}^{1+}(4s^1)$	$\text{Zn}^0(4s^2)$
1s	16 116.32	16 116.24	16 116.20	-0.11	-0.17
2s	1 639.15	1 639.33	1 639.42	+0.25	+0.38
3s	234.31	234.85	235.14	+0.76	+1.16
4s	0.00	6.14	9.11	+8.60	+12.75
Total	17 989.78	17 996.56	17 999.87	+9.49	+14.13

and Zn^0 have, respectively, one and two $4s$ electrons outside the $\text{Ar}3d^{10}$ core. The Dirac-Fock calculations⁴⁰ are numerical without any basis set restrictions while the atomic Hartree-Fock calculations use the same Gaussian basis set,^{38,39} namely, the $\text{Zn}(8s6p2d)$: (62111111/511111/41) contraction described earlier, which is employed for all of the cluster calculations. Comparison of the numerical Dirac-Fock and analytic Gaussian basis set Hartree-Fock results allows a test of the suitability of this basis set for $\rho(0)$ calculations. First of all, taking the ratio of the total Dirac-Fock density $|\psi(0)|^2$ to the total Hartree-Fock contact density $\rho(0)$ gives a scaling factor $S'(Z)$ equal to 1.393 which is quite close to the accepted value of 1.40, the value used throughout this study. Perhaps a more important test is the trend in the individual atomic-orbital contributions to $\Delta\rho(0)$ as the $\text{Zn}(4s)$ population increases in going from the Zn^{2+} to the Zn^0 configuration. One observes from Table II that the variation in contact density between the Dirac-Fock $\Delta|\psi(0)|^2$ and the Hartree-Fock $S'(Z)\Delta\rho(0)$ follow each other in both magnitude and sign as the $\text{Zn}(4s)$ population increases. These results demonstrate the suitability of both the chosen Zn basis set and the approximation of scaling the Hartree-Fock density by a constant factor $S'(Z)$ to adequately reproduce the changes in the relativistic contact density.

As described above, the chosen cluster is embedded in a point-charge array to include the Madelung potential from the infinite solid. In regard to the choice of what charge values to use in the embedding lattice we have considered two cases. The first choice is to use formal charges. Thus, since we are dealing with binary crystals, for ZnO , ZnS , ZnSe , and ZnTe , the magnitudes of the formal charges should be equal, for example, +2 for Zn and -2 for S, assuming total ionicity for ZnS , while for ZnF_2 , the zinc charge is two times the fluorine charge in order to give charge neutrality for the solid. The second choice is to use charges that reflect the extent of covalent bonding obtained from our calculations. In this respect, since the central zinc atom is best described within the cluster due to this atom being fully coordinated by its nearest-neighbor ligands within the cluster rather than considering them as external point charges, the charge on the central zinc atom, obtained from a population analysis, for example, can be used to determine the charges for the external point-charge array. A charge self-consistent procedure is possible where the external

point charges are initially assumed to be fully ionic. A Mulliken population analysis⁴¹ on the self-consistent cluster molecular orbitals yields the gross orbital populations for the cluster sites from which the Mulliken charge for the central zinc atom is obtained. Next, the external point charges are replaced by new point-charge values using the zinc Mulliken charge as a guide. The ligand point-charge values are determined from the zinc Mulliken charge as well, since the zinc atom is fully coordinated by ligands within the cluster. The Hartree-Fock cluster procedure is repeated with these new external point charges. This procedure can be repeated until the resulting zinc Mulliken charge is equal to the zinc charge of the external point ions. This process of charge iteration to self-consistency converges very quickly, with the Mulliken zinc charge approaching the external charge value to within about 0.02 after just one cycle.

The two sets of results obtained through these two procedures provide an estimate of the sensitivity of the electronic properties to the choice of point charges used for the rest of the lattice outside the cluster. As an example, the use of formal point charges with the $(\text{ZnS}_4)^{6-}$ cluster representative of ZnS yields a Zn Mulliken charge of +1.45. Then, the external point charges which originally were +2 at Zn sites and -2 at S sites are replaced by charges of +1.45 and -1.45 for Zn and S point ions. We then compare the calculated charge densities $\rho(0)$ at the central zinc nucleus using both formal charges and Mulliken charges for the external point ions (see Table III). The difference in these two results is considered as a measure of the influence of the process of incorporation of the rest of the lattice outside the cluster on the confidence limits of $\rho(0)$ and $\Delta\rho(0)$.

Finally, one should consider the influence of the second-order Doppler effect on the measured center shifts⁵⁻⁷ in Mössbauer experiments. The experimentally measured Mössbauer center shift S_C is actually the sum of two distinct quantities, the isomer shift S which is related to the electron density at the nucleus by Eq. (2) and the second-order Doppler effect S_{SOD} due to the vibrating motion of the ^{67}Zn atom around its equilibrium position in the lattice. As a consequence of the relatively light mass, the high-resonance energy, and extremely narrow linewidth, one should not assume the S_{SOD} is negligible in comparison to the isomer shift. Because of the zero-point motion this is true also at low temperatures (4.2 K and

TABLE III. Total charge densities at the zinc nucleus, $\rho(0)$.

System	Zn Mulliken charge	$\rho(0)(a_0^{-3})$ (Formal charges) ^a	$\rho(0)(a_0^{-3})$ (Mulliken charges) ^b
ZnF_2 (F^0 basis)	1.68	17 991.41	17 991.44
ZnF_2 (F^1 basis)	1.85	17 991.40	17 991.41
ZnO (rocksalt)	1.65	17 991.94	17 991.86
ZnO (wurtzite)	1.62	17 992.69	17 992.76
ZnS	1.45	17 993.67	17 993.67
ZnSe	1.37	17 993.87	17 993.85
ZnTe	1.34	17 994.41	17 994.35

^aFormal charges.

^bMulliken charges are used for the ionic charges outside the cluster.

below) where most of the ^{67}Zn Mössbauer measurements have been performed. The quantity S_{SOD} is proportional to the mean-square velocity $\langle v^2 \rangle$ of the ^{67}Zn nucleus. The change of S_{SOD} between two different absorbers has until now been determined in the literature⁵⁻⁷ by measuring the mean-square displacement $\langle x^2 \rangle$ of the nucleus as obtained from the recoil-free fraction and then relating this measurement to $\langle v^2 \rangle$ by the Debye model. The assumption of a Debye solid may, however, not be accurate enough for the binary zinc compounds investigated here as suggested by the disagreement⁵ in values predicted for the specific heats for the zinc chalcogenides and ZnF_2 as compared to the experimental data. We have, therefore, used S_{SOD} for each compound as evaluated in Ref. 5 with the help of lattice-dynamic calculations using the force constants of appropriate shell models. For ZnTe , ZnSe , ZnS , and ZnO , respectively, the models of Refs. 42, and 43, and for ZnF_2 of Ref. 44, were employed. The second-order Doppler shift S_{SOD} is given by⁵

$$S_{\text{SOD}} = -\frac{\hbar}{2m_{\kappa}cN} \sum_{\mathbf{q}j} \omega(\mathbf{q}) \cdot |\mathbf{e}(\kappa|\mathbf{q},j)|^2 \left[n_j(\mathbf{q}) + \frac{1}{2} \right], \quad (3)$$

where \mathbf{q} is the wave vector for the phonon, c is the vacuum velocity of light, κ labels the ^{67}Zn site within the unit cell, m_{κ} is the mass of the ^{67}Zn atom. The eigenvectors $\mathbf{e}(\kappa|\mathbf{q},j)$ indicate the polarization of the mode (\mathbf{q},j) associated with the eigenfrequency $\omega_j(\mathbf{q})$. N is the number of unit cells of the finite crystal. The phonon occupation number $n_j(\mathbf{q})$ at temperature T is given by

$$n_j(\mathbf{q}) = \left[\exp \left(\frac{\hbar\omega_j(\mathbf{q})}{k_B T} \right) - 1 \right]^{-1}, \quad (4)$$

where k_B is the Boltzmann constant.

We want to emphasize that both the eigenvalues and the eigenvectors are needed to determine S_{SOD} . Therefore, in Ref. 5, the eigenvalue problem of the dynamic matrix was solved and used to calculate S_{SOD} according to Eqs. (3) and (4). Using these values of S_{SOD} , we derived S from the measured center shifts S_C for each compound.⁷⁻¹² The values for the measured S_C , the calculated S_{SOD} , and the isomer shift which is the difference of S_C and S_{SOD} are listed in Table VII with ^{67}ZnO (wurtzite) as the reference compound.

III. RESULTS AND DISCUSSION

Table I gives the structures and lattice constants of the compounds investigated here. The Hartree-Fock cluster procedure is then applied to these systems to obtain self-consistent cluster molecular orbitals from which $\rho(0)$ is calculated. Table III gives our results for the charge densities $\rho(0)$ at the zinc nucleus for all of the systems and, in the case of ZnF_2 with basis sets optimized for both neutral and ionic fluorine. The results of these calculations are given for two situations: (i) where the external point charges are assumed to have their formal totally ionic values, and (ii) where the Mulliken charges are used for the external charges, as discussed in Sec. II. Qualitatively, one observes that $\rho(0)$ increases with decreasing Pauling electronegativity of the ligand and also that the

Mulliken charge on the central zinc atom decreases with increasing $\rho(0)$. These trends follow the experimental observation⁷ that the isomer shift decreases with increasing Pauling electronegativity of the ligand. In Fig. 1 we plot the experimental isomer shifts and the theoretically derived contact densities against the Pauling electronegativity difference between the ligand and zinc. For the octahedrally coordinated compounds, since the electronegativity differences may be considered to represent values of the electronegativity difference per bond, this Pauling electronegativity difference is scaled by an empirical factor of 1.5 to account for the 1.5 times greater number of nearest-neighbor Zn-ligand bonds in the octahedral systems, ZnO (rocksalt), and ZnF_2 , as compared to the tetrahedrally coordinated compounds. One should note the high degree of linearity in the dependence between the electronegativity and the isomer shifts or electron densities. These trends suggest that the isomer shift appears to be dominated by contact density variations arising predominantly from the valence orbitals as opposed to the core orbitals. However, a detailed analysis is required to check this intuition since it is conceivable that the valence electrons could, through their influence on the core electrons, transfer the change associated with

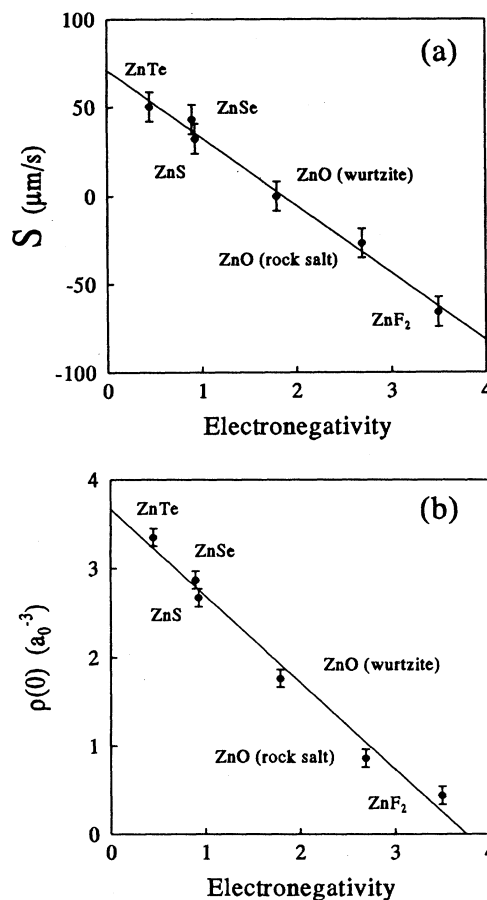


FIG. 1. Plots of (a) the experimental isomer shifts with respect to $^{67}\text{GaZnO}$ (wurtzite) and (b) the charge density at the zinc nucleus with respect to a constant density of $17991a_0^{-3}$, against Pauling electronegativities.

them to the core electrons. The conclusion that valence electrons are directly responsible for the isomer shift can only be obtained from an analysis of the various valence-like and corelike contributions to the change in contact density. This is done later in this section.

The significant difference observed between the Zn Mulliken charges for ZnF₂ using the F⁰ and F¹⁻ basis sets is likely a result of the way that the Mulliken population analysis⁴¹ divides charge between overlapping atomic orbitals. This type of population analysis assigns charge equally between overlapping atomic orbitals which leads to a basis set dependence. It is known⁴⁵ that Mulliken charges should only be considered as qualitative in significance and only charges from similarly constructed basis sets should be used for direct comparison of Mulliken charges. Hence, from Table III in comparing the Zn Mulliken charge for ZnF₂ to the other systems listed, it is advisable to consider the F⁰ basis set results since all the other basis sets have been optimized for neutral atoms. Most important, it can be seen from Table III that there is very little difference in $\rho(0)$, related directly to the isomer shift, whether the F⁰ or the F¹⁻ basis set is used in the calculation.

From Table III, one generally observes little variation in $\rho(0)$ when either formal or Mulliken charges are used in the external point-charge lattice. The greatest variation occurs with ZnO (rocksalt) where $\rho(0)$ decreases by $0.08a_0^{-3}$. The average magnitude of variation between the use of formal versus Mulliken charges over all the systems studied is only $0.04a_0^{-3}$. These results show that the differences in calculated electron density due to the two different choices of point-charge values in the external point ion lattice are relatively small compared to the changes in $\rho(0)$ among the different solids. Thus, using the density differences between the choice of formal or Mulliken charges for the external point charges as a measure of uncertainty in our calculated $\rho(0)$ values gives a conservative estimate of $0.08a_0^{-3}$ in the confidence limit for the calculated nonrelativistic electron density at the nucleus. This would amount to a contribution to the confidence limit of about $0.12a_0^{-3}$ in the relativistic density. On augmenting this by an estimate of the computational error range involved in the calculation, one can make a conservative estimate of about $0.2a_0^{-3}$ for the net contribution of the calculated electron density to the confidence limit of our results.

It is possible to estimate the individual atomic-orbital contributions of zinc to $\rho(0)$ by inspection of the atomic characters of the individual cluster molecular orbitals.

The contribution from the core orbitals is relatively simple due to their wide energy separations and negligible mixing with other atomic orbitals. The valence molecular orbitals are more difficult to analyze but the total valence contribution to $\rho(0)$ is assigned to the molecular orbitals which involve the Zn(4s)-like atomic orbitals since the Zn(3s) molecular orbital is much lower in energy. In Table IV we present our results for the contributions due to Zn(1s), Zn(2s), Zn(3s), and the Zn(4s) orbitals using this procedure. These assignments represent the net contributions from all the occupied cluster orbitals. The core Zn(1s), Zn(2s), and Zn(3s) orbital contributions arise from a single molecular orbital, each with approximately 100% Zn(s)-like character indicating that these orbitals are atomiclike. The Zn(4s) contribution to $\rho(0)$ involves more than one valence molecular orbital; a more detailed discussion about this will be given later in this section. From Table IV one observes several trends in going from ZnF₂ to ZnTe corresponding to decreasing electronegativity of the ligand and expected decreasing ionicity of the chemical bond. First, the Zn(1s) contribution decreases by $0.14a_0^{-3}$ while the Zn(2s) contribution to $\rho(0)$ increases by $0.10a_0^{-3}$. Thus, the contributions to $\Delta\rho(0)$ due to Zn(1s) and Zn(2s) orbitals nearly cancel each other. Next, the change in $\rho(0)$ in going from ZnF₂ to ZnTe are, respectively, $+0.62a_0^{-3}$ for Zn(3s) and $+2.36a_0^{-3}$ for Zn(4s) orbitals. This indicates that the major contribution to $\Delta\rho(0)$ comes from the valence orbitals. However, the role of the Zn(3s) orbital should not be neglected since its contribution to $\Delta\rho(0)$ is approximately 20% of the total variation.

It is interesting to inquire into the causes for the contributions to $\Delta\rho(0)$ from the core electrons. The possible factors that could lead to the core contributions to $\Delta\rho(0)$ are (a) the influence of the additional potential due to the different charges on the neighboring ions of zinc, both from the ions within the cluster and outside, (b) the changes in the potential seen by the core electrons due to changes in the populations of the valence electron states of zinc including the 3d, 4s, and 4p shells, (c) the Pauli or overlap repulsion⁴⁶ of the core electrons by the electrons on the ligands, and (d) covalent bonding of the core electrons with the ligand electrons. All of these effects are, of course, included in our investigations, but it is interesting to attempt to assess the relative importance of these various contributions to the core electron contact density.

First, consider the increase in $\rho(0)$ from the 3s electron in Table IV in going from ZnF₂ which has six nearest singly charged F¹⁻ neighbors to ZnO with the rocksalt

TABLE IV. Individual contributions to $\rho(0)$ in units of a_0^{-3} .

Orbitals	$\rho(0)(a_0^{-3})^a$					
	ZnF ₂	ZnO (rocksalt)	ZnO (wurtzite)	ZnS	ZnSe	ZnTe
Zn(1s)	16 116.25	16 116.22	16 116.17	16 116.13	16 116.13	16 116.11
Zn(2s)	1 639.11	1 639.13	1 639.14	1 639.18	1 639.19	1 639.21
Zn(3s)	234.25	234.34	234.45	234.73	234.76	234.87
Zn(4s)	1.80	2.17	3.00	3.63	3.77	4.16

^aMulliken charges are used for the external charges. For ZnF₂, only the results using the F¹⁻ basis set for fluorine ligand are shown.

structure which has six doubly charged O^{2-} neighbors. The larger density at the zinc nucleus from the 3s electrons when one goes from the free ion (Table II) to the ionic crystals clearly argues against the causes (a) and (d). Addressing first the cause (a), because the potential from the negative ions would lead to a weaker potential for the 3s core electrons, one would expect a reduction in the density at the nucleus as compared to the free ion. In fact, the opposite trend is observed. The same remark applies to the expected and observed trends due to cause (a) in going from the stronger repulsive Coulomb potential from the doubly charged O^{2-} ion as compared to the F^{1-} ion in comparing ZnF_2 with the cubic ZnO system. As far as cause (d), involving covalent bonding between the zinc core electrons and ligand electrons, is concerned, any such bonding would lead to a decrease in the density at the nucleus while an increase is actually observed in going from the free ion to the chalcogenides ZnO through ZnTe . The same remark applies in going from ZnF_2 to ZnO (rocksalt), the covalent bonding being expected to be stronger in the latter system.

In attempting to assess the importance of the other two mechanisms (b) and (c), we shall consider first the former, namely, the relaxation or alteration of the core state wave functions due to the change in the population in the valence states of the zinc due to covalent bonding with the ligand orbitals. This leads to a change in the valence electron density on the zinc atom and a consequent change in the potential experienced by the core electrons. Thus, considering, for example, the three systems ZnF_2 , ZnS , and ZnTe the calculated zinc *s*, *p*, and *d* Mulliken electron populations in these systems came out as *s*:(6.20, 6.34, 6.36), *p*:(12.12, 12.23, 12.32), and *d*:(10.00, 9.98, 9.98), respectively. These numbers show that the electronic populations in each of these systems is a fraction of an electron larger than 28, leading one to expect that the effective charges are between 2 and 1, corresponding to Zn^{2+} and Zn^{1+} as has been shown in Table III. These electron populations also show that in going from ZnF_2 to ZnTe , the *s*, *p*, and *d* populations increase by 0.16, 0.20, and -0.02 , respectively. Results are available for the electron contact densities from different core and valence states for the $\text{Zn}^0(3d^{10}4s^14p^1)$ configuration from Dirac-Fock calculations.⁴⁰ On comparing the 3s core density for this configuration with that for the $\text{Zn}^{1+}(3d^{10}4s^14p^0)$ configuration listed in Table II, the value of $\Delta|\psi_{3s}(0)|^2$ corresponding to the density difference with respect to the $\text{Zn}^{2+}(3d^{10}4s^04p^0)$ configuration changes from 0.85 for $4p^0$ population to 0.89 for $4p^1$, that is, a difference in $\Delta|\psi_{3s}(0)|^2$ corresponding to $0.04a_0^{-3}$. On weighting this result with the change of 4*p* population of 0.2 electrons found from our cluster calculations between ZnF_2 and ZnTe , we expect a density change of only 0.008 from the change in 4*p* population due to change in the covalent bonding. Correspondingly, applying the weighting factor of 0.16 for the change in 4*s* population in going from ZnF_2 to ZnTe and the difference in $\Delta|\psi_{3s}(0)|^2$ of 0.85 between the $\text{Zn}^{2+}(3d^{10}4s^04p^0)$ and $\text{Zn}^{1+}(3d^{10}4s^14p^0)$ configurations listed in Table II, one estimates an expected change of 0.136 in going from ZnF_2 to ZnTe due to cause (b) involv-

ing relaxation in the 3s orbital due to changes in the 4s population. The corresponding change in $\Delta|\psi_{3s}(0)|^2$ due to a change in 3*d* population is expected to be negligible, both because of the very small population change (-0.02 electrons) found for the 3*d* electrons and also because the change in 3s density due to a variation in 3*d* population is expected to be even weaker than for the 4*p* population, since the former has a smaller density in the internal regions of the ion. Thus, the net change due to cause (b) in $\Delta\rho_{3s}(0)$ is about 0.14 as compared to the change of 0.62 found from the results of our cluster calculations in Table IV which translates to $0.87a_0^{-3}$ on applying the relativistic enhancement factor of 1.4 discussed earlier. Thus, while the relaxation of the core orbitals due to changes in the valence electronic populations on the Zn^{1+} ion makes a contribution to $\Delta|\psi_{3s}(0)|^2$ in the right direction as the net change found from our cluster calculations, this contribution is substantially smaller, by more than a factor of 6. One, therefore, has to ascribe the major cause for the change in $\Delta|\psi_{3s}(0)|^2$, and, indeed, the $\Delta|\psi_{1s}(0)|^2$ and $\Delta|\psi_{2s}(0)|^2$ to the cause (c) involving overlap repulsion between the ligand electrons and core electrons of zinc leading to enhanced core density at the zinc site. The trend of increase in $\Delta\rho_{3s}(0)$ and $\Delta\rho_{2s}(0)$ seen from Table IV, as one goes from the F^{1-} ligand ion to the increasingly diffuse ligand ions from O^{2-} to Te^{2-} is in keeping with the overlap repulsion model, as is also the much weaker effect for the tightly bound 2s electrons as compared to 3s. The reversal in the trend of the small variation in $\Delta\rho_{1s}(0)$ as compared to $\Delta\rho_{2s}(0)$ and $\Delta\rho_{3s}(0)$ in going from the fluoride to the telluride could also be a result of the indirect influence on the 1s orbital of the increase in 2s and 3s contact densities by the overlap repulsion effect. The effect (a) for $\Delta\rho_{1s}(0)$, while apparently in the right direction from Table II, is expected to be much smaller than the observed decrease of 0.14 in going from ZnF_2 to ZnTe (as seen from Table IV from the cluster calculations) by the same arguments concerning the changes in 4s and 4*p* populations used in discussing $\Delta\rho_{3s}(0)$.

The dominant contribution to $\Delta\rho(0)$ comes from the valence molecular orbitals. Therefore, before discussing the nature of the agreement between theory and experiment it is helpful to analyze those aspects of the electronic structure which are important to the valence contribution to $\Delta\rho(0)$. We shall first consider the tetrahedrally coordinated systems ZnO (wurtzite), ZnS , ZnSe , and ZnTe and subsequently the two octahedrally coordinated systems, namely, ZnO (rocksalt) and ZnF_2 . For analysis of the electronic structures, we have chosen, for brevity, to discuss just the results obtained using the Mulliken charges for the external point ions though most aspects of the electronic structure remain the same when formal charges are used for the ions. The only significant difference is that since the Madelung potential is reduced when the smaller Mulliken charges are used compared to the formal charges, the energy levels are higher in energy for the former case. This can be seen in Fig. 2 for ZnS and is due to the shallower potential well for the Mulliken charge case as compared to the formal charge case. The smaller Mulliken charges reflect qualitatively increased covalency as compared to the total ionicity as-

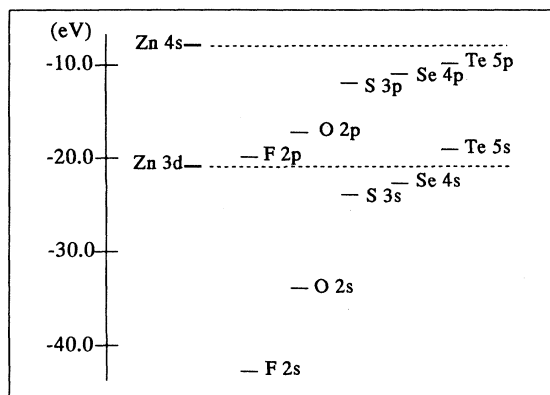


FIG. 4. Hartree-Fock atomic energy levels for Zn, F, O, S, Se, and Te neutral atoms.

emission spectroscopy experiments⁴⁷ which attest to the correctness of the approximations of the cluster procedure and the cluster sizes chosen. In regard to the $\rho(0)$ calculations, our results should not be significantly affected by the discrepancy in ZnTe, since T_d point symmetry does not allow mixing between Zn($3d$) and Zn(s) atomic orbitals. The molecular orbitals responsible for $\rho(0)$ for the $(\text{ZnTe}_4)^{6-}$ cluster only involve Zn(s) and Te(s, p, d) atomic orbitals. The Zn($3d$) is not likely to be involved in the isomer shift for ZnTe except through possible screening effects of the Zn(s) electrons by the Zn($3d$) electrons. This should be a small effect for the zinc chalcogenides since the indirect effect on $\Delta\rho(0)$ from the valence electrons due to screening by Zn(d) or Zn(p) electrons, especially the former, is in general expected to be small compared to the direct contribution to $\rho(0)$ from the Zn(s) electrons by arguments similar to those made earlier in discussing the trends of the core contributions in going from ZnF₂ to ZnTe.

Table V lists the valence cluster orbitals and their ap-

proximate percentage atomic-orbital characters which significantly contribute to the valence $\rho(0)$. The Zn(p) character of these orbitals is all zero as expected. For the tetrahedral clusters representative of ZnO (wurtzite), ZnS, ZnSe, and ZnTe two molecular orbitals each make a substantial contribution to $\rho(0)$. The higher in energy of these two is the $11a_1$, $8a_1$, $10a_1$, and $12a_1$ orbital, respectively, for ZnO (wurtzite), ZnS, ZnSe, and ZnTe. As observed from Table V this orbital gives the largest contribution to the valence $\rho(0)$, and, therefore, is the most important orbital for $\Delta\rho(0)$ and the experimental isomer shifts across the whole series of compounds. Also, this orbital is the lowest in energy of the ligand(p)-like orbitals and, as seen from the approximate percent characters, has substantial covalent mixing. In going from ZnO (wurtzite) to ZnTe, and Zn($4s$) character increases from 12.0 to 20.4%, the ligand(d) character increases from less than 0.1 to 0.5% while the ligand(p) character decreases from 87.4 to 70.8%. These trends indicate the covalent mixing within this orbital increases as one goes through the series of compounds from ZnO (wurtzite) to ZnTe. One also notices that an increase in Zn(s) character of the orbital corresponds to an increase in $\rho(0)$ for that orbital. Since this orbital involves substantial covalent mixing between Zn(s)-like and ligand(p)-like atomic orbitals and no other molecular orbitals share this characteristic, we surmise that this orbital is likely the sp bonding orbital, between the Zn($4s$) and valence ligand(p) atomic orbitals, for these clusters. Therefore, this molecular orbital corresponds to the sp bonding orbitals of the zinc chalcogenide compounds. Since this molecular orbital gives the greatest relative contribution to $\Delta\rho(0)$, our cluster calculations predict that to a large extent ^{67}Zn Mössbauer isomer-shift experiments sample the Zn($4s$) character of the sp bonding orbitals for the zinc chalcogenides. Finally, an interesting feature of the ZnS $8a_1$, ZnSe $10a_1$, and ZnTe $12a_1$ molecular orbitals is the relatively small participation of the ligand valence d

TABLE V. List of valence molecular orbitals which give the greatest contributions to $\rho(0)$.

System	Cluster orbital	Energy (eV)	$\rho(0)$ (a_0^{-3})	(Approximate % atomic character of orbital)				
				Zn(s)	Zn(d)	Ligand(s)	(p)	(d)
ZnF ₂	$11a_g$	-15.52	0.07	1.1	9.8		89.0	
	$10a_g$	-16.42	1.58	5.3	3.8	0.4	90.5	
	$6a_g$	-39.47	0.14	0.3		99.7		
ZnO (rocksalt)	$6a_{1g}$	-4.83	1.95	8.1		0.6	91.3	
	$5a_{1g}$	-22.83	0.22	4.5		95.3	0.2	
ZnO (wurtzite)	$11a_1$	-7.13	2.66	12.0	0.1	0.5	87.4	
	$8a_1$	-25.38	0.52	1.9		97.8	0.3	
ZnS	$8a_1$	-5.97	3.11	17.9		2.1	79.8	0.2
	$7a_1$	-17.33	0.52	2.1		97.4	0.5	
ZnSe	$10a_1$	-5.18	3.23	19.8		3.1	76.9	0.2
	$9a_1$	-15.92	0.54	2.2		97.3	0.5	
ZnTe	$12a_1$	-5.86	3.34	20.4		8.3	70.8	0.5
	$11a_1$	-14.01	0.82	3.1		96.5	0.4	

electrons in these orbitals. While empty in free atoms, the S(3*d*), Se(4*d*), and Te(5*d*) electrons are shown here to be involved, albeit fairly weakly, in the cluster orbital responsible for the largest variation in $\rho(0)$ in these systems. In order to quantitatively investigate the importance of the valence ligand *d* states to the contact density we have repeated cluster calculations for ZnF₂, ZnO (wurtzite), ZnS, and ZnTe with ligand basis sets without *d*-polarization functions. These *d*-polarization functions partially describe the valence ligand *d* states as discussed in Sec. II. Using ligand basis sets without *d*-polarization functions, the calculated contact densities for ZnF₂, ZnO (wurtzite), ZnS, and ZnTe were reduced by respectively 0.02, 0.03, 0.33, and $0.28a_0^{-3}$, suggesting that the valence *d* states in S, Se, and Te contribute roughly $0.3a_0^{-3}$, while the F(3*d*) and O(3*d*) valence states contribute a factor of 10 smaller to the contact density.

A second cluster orbital gives a smaller but still significant contribution to the valence $\rho(0)$. Thus, from Fig. 4 and Table V the orbitals labeled as $8a_1$, $7a_1$, $9a_1$, and $11a_1$ in ZnO (wurtzite), ZnS, ZnSe, and ZnTe are also important contributors to $\rho(0)$. Their contributions are nearly constant for the series ZnO (wurtzite), ZnS, and ZnSe ranging from 0.52 to $0.54a_0^{-3}$, while for ZnTe this orbital contributes $0.82a_0^{-3}$ to $\rho(0)$. From Table V it is seen that this orbital is mainly of ligand(*s*)-like character. As one goes through the series ZnO (wurtzite) to ZnTe, the amount of Zn(4*s*) character increases while the ligand(*s*) character decreases corresponding to increased covalent mixing.

Figure 5 presents the one-electron energy levels for the $(\text{ZnF}_6)^{4-}$ and $(\text{ZnO}_6)^{10-}$ clusters for ZnF₂ and ZnO (rocksalt). The $(\text{ZnO}_6)^{10-}$ cluster has perfect octahedral O_h point symmetry while the $(\text{ZnF}_6)^{4-}$ cluster as a consequence of the tetragonal nature of the ZnF₂ crystal, is distorted to D_{2h} symmetry. As with the tetrahedrally coordinated clusters, the lowest unoccupied molecular orbital has mainly Zn(4*s*)-like character. The valence energy levels are also clustered into three distinct groups as before. The uppermost group has primarily ligand(2*p*)-like character, the intermediate group has mainly Zn(3*d*)-like character, and the lowest energy group has mainly ligand(2*s*)-like character. Just as with the tetrahedrally coordinated clusters, the lowest-energy orbital in the ligand(2*p*)-like group is the dominant contributor to the valence $\rho(0)$ with a smaller contribution from the lowest-energy ligand(2*s*)-like orbital. For ZnO (rocksalt) these two orbitals are labeled as $6a_{1g}$ and $5a_{1g}$, their approximate atomic characters being given in Table V. For ZnF₂, there are actually two orbitals which give significant contributions to the valence $\rho(0)$ from the uppermost ligand(*p*)-like group of orbitals, namely, $10a_g$ and $11a_g$. An interesting feature of the $10a_g$ and $11a_g$ orbitals for ZnF₂ is the substantial Zn(3*d*)-like atomic character in the bond. This mixing is allowed due to the relatively low D_{2h} symmetry (Zn *d*_z² orbitals transform according to the *a_g* irreducible representation of the D_{2h} point group) of the $(\text{ZnF}_6)^{4-}$ cluster and the relative closeness of the Zn(3*d*) and F(2*p*) atomic energies which can be seen in Fig. 4. ZnF₂ has a relatively high degree of

Zn(3*d*)-ligand(*p*) hybridization in comparison to all the other compounds studied here. These observations show the importance of having an accurate description of the Zn(3*d*) orbitals for a reliable calculation of $\rho(0)$ in ZnF₂. In particular, the Zn(3*d*) orbitals should not be treated in the frozen-core approximation for a calculation of $\rho(0)$ in ZnF₂. In regards to all-electron Hartree-Fock cluster calculations, this means that the Zn(3*d*) portion of the basis set should have strong variational flexibility.

Due to the relative importance of fluorine(2*p*)-zinc(3*d*) mixing for the contact density in ZnF₂, it is interesting to inquire about the general trend in this *pd* mixing for the whole series of compounds investigated. We can obtain an estimate of the amount of ligand(*p*)-Zn(3*d*) hybridization in the binary zinc compounds from comparisons of the atomic percentage characters of the highest occupied molecular orbital in these systems. In going through the series ZnF₂, ZnO (rocksalt), ZnO (wurtzite), ZnS, ZnSe, and ZnTe, the highest occupied molecular orbital has, respectively, approximately 18.3, 10.0, 8.8, 2.8, 2.0, and 1.2% Zn(*d*)-like atomic character. In this same series the ligand(*p*)-like percent atomic characters are, respectively, 81.4, 89.2, 90.3, 93.7, 92.9, and 92.6. Taking the ratio of these two characters as a qualitative measure of the degree of Zn(3*d*)-ligand(*p*) mixing gives 0.23, 0.11, 0.10, 0.03, 0.02, and 0.01 for, respectively, ZnF₂, ZnO (rocksalt), ZnO (wurtzite), ZnS, ZnSe, and ZnTe. One

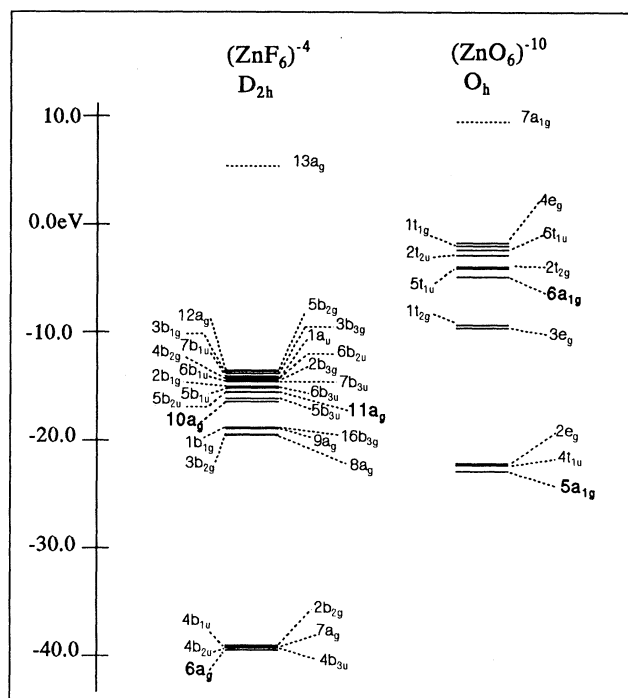


FIG. 5. Valence one-electron energy levels for the clusters used to represent ZnF₂ and ZnO (rocksalt). The cluster orbitals are labeled according to the irreducible representations of the D_{2h} and O_h point groups [orbitals important to $\rho(0)$ are highlighted in bold]. The external point ions are taken from the Mulliken analysis.

observes that there is substantial pd mixing of this type for ZnF_2 . The amount of pd mixing is about half as great but still significant for ZnO (rocksalt) and ZnO (wurtzite). For ZnS , ZnSe , and ZnTe there is much less pd mixing in comparison to either ZnF_2 or ZnO . These trends qualitatively follow the trends in atomic energy differences given in Fig. 4 between the $\text{Zn}(3d)$ ligand(p) atomic energy levels.

In summary, for the binary zinc compounds ZnF_2 , ZnO (rocksalt), ZnO (wurtzite), ZnS , ZnSe , and ZnTe , the dominant contribution to $\Delta\rho(0)$ at the zinc nucleus comes from the $\text{Zn}(4s)$ molecular orbitals. A smaller, though certainly non-negligible, contribution is due to the shallow core $\text{Zn}(3s)$ molecular orbital. The variations in the $\text{Zn}(3s)$ density at the nucleus among the different compounds is seen from Table IV to follow the variation in the population of the valence Zn , especially the $\text{Zn}(4s)$, orbitals. This result is not unexpected because the repulsive effect of the ligand electrons, which has been analyzed above to be the main contributor to the change in $\Delta\rho(0)$ from the core electrons, increases in importance as the ligand electrons become more diffuse in going from ZnF_2 , ZnO , to ZnTe . This diffuseness is expected to lead to greater charge transfer to the $4s$ orbital of the Zn^{2+} ion through covalent bonding and hence, a greater valence contribution to $\Delta\rho(0)$. Also, we have shown that the major contribution to the valence $\Delta\rho(0)$ comes from the zinc-ligand bonding molecular orbital(s).

In our present investigations, many-body correlation effects have not been included. However, there is evidence from careful many-body perturbation theoretic investigations⁴⁹ on the Fe^{3+} ion that these effects are relatively weak in influencing electron-density differences at the nucleus. Additionally, recent many-body investigations⁵⁰ in a number of small molecular systems containing iron have also shown the relative unimportance of correlation effects for the isomer shift. We shall therefore consider our results for $\Delta|\psi(0)|^2$ to represent quite accurately the actual density differences between the zinc compounds considered here.

The calculated $\rho(0)$ values and the experimental isomer shifts increase with increasing covalent mixing of the Zn -ligand bond. This is in accord with the observation that both the derived $\rho(0)$ and the experimental isomer shifts decrease with increasing Pauling electronegativity of the ligand. From Eq. (2), these trends predict that the nuclear parameter $\Delta\langle r^2 \rangle$ is positive for ^{67}Zn . Having demonstrated that the trends in the electron densities at the nuclei are in keeping with the experimental isomer-shift data, and that a number of features of the electronic energy levels and wave functions are in agreement with experiment, we shall now consider the results one obtains for the nuclear parameter $\Delta\langle r^2 \rangle$ involving the difference in nuclear density distributions in the excited and ground Mössbauer nuclear states, using our calculated electron contact densities for the binary zinc compounds studied in this work. Comparison with the known³³ experimental value for $\Delta\langle r^2 \rangle$ provides a quantitative test of the calculated contact densities. Before the actual derivation of $\Delta\langle r^2 \rangle$ with our results, it is instructive to review a simple physical picture and the assumptions involved concern-

ing the correct sign for this quantity. A positive value for $\Delta\langle r^2 \rangle$ simply means that the first excited Mössbauer nuclear state has a mean-square radius larger than the ground state.

The sign of $\Delta\langle r^2 \rangle$ for the 93.3 keV Mössbauer transition for ^{67}Zn is unambiguously positive. This has been demonstrated not only by recent experiments but can also be justified by a simple physical argument. It is interesting to note that this physical picture actually predicted⁷ the correct sign before any first-principles calculations or electron-capture experiments were available. There is a clear linear trend observed⁷ between the isomer shifts and Pauling electronegativity of the ligand as can be seen in Fig. 1. Since the zinc chalcogenides are primarily sp bonded systems,⁵¹ the electron density at the zinc nucleus arising from the $\text{Zn}(4s)$ orbitals is expected to decrease with increasing electronegativity of the ligand with zinc tending more toward a Zn^{2+} ion configuration. Thus, the decrease in isomer shift with increasing electronegativity indicates from Eq. (2) that $\Delta\langle r^2 \rangle$ is positive. This argument, along with our calculations, indicates that the variations in $\rho(0)$ are of a chemical nature, relating to the degree of covalent mixing between valence $\text{Zn}(4s)$ and valence ligand atomic orbitals. The major contribution to $\Delta\rho(0)$ has been shown from discussions earlier in this section to arise from the molecular orbitals involving $\text{Zn}(4s)$.

The results from Table VI showing the calculated $\rho(0)$ values scaled by $S'(Z)=1.40$ and the experimental isomer shifts^{5,8-10} listed in Table VII are plotted in Fig. 6. The isomer shifts are given with respect to $^{67}\text{GaZnO}$ (wurtzite). As discussed previously, the constant scale factor $S'(Z)=1.40$ is required in order to correct for employing nonrelativistic rather than relativistic density differences. As seen from Fig. 6, there is a high linear correlation between the calculated charge densities and the experimental isomer shifts. This good linearity attests to the accuracy of our calculated contact density differences for the binary zinc compounds investigated here. The slope of the straight-line fit through this data combined with Eq. (2) gives the calculated value of $\Delta\langle r^2 \rangle = +13.9 \times 10^{-3} \text{ fm}^2$ with a confidence limit of approximately 10%. The confidence limit is based on the error range of about $8.3 \mu\text{m/s}$ in all S values, originating mainly from the evaluations of S_{SOP} and from the uncertainties of about $\pm 0.2a_0^{-3}$ in $\Delta|\psi(0)|^2$ from various sources described earlier. This result is in reasonable

TABLE VI. Electron densities $|\psi(0)|^2$ at the Zn nucleus.

System	$ \psi(0) ^2(a_0^{-3})^a$ (Formal charges)	$ \psi(0) ^2(a_0^{-3})^a$ (Mulliken charges)
ZnF_2 (F^{-1} basis set)	25 187.96	25 187.97
ZnO (rocksalt)	25 188.72	25 188.60
ZnO (wurtzite)	25 189.77	25 189.86
ZnS	25 191.14	25 191.14
ZnSe	25 191.42	25 191.39
ZnTe	25 192.17	25 192.09

^a $|\psi(0)|^2 = S'(Z)\rho(0)$ with $S'(Z)=1.40$.

TABLE VII. Experimental center shifts S_C , calculated S_{SOD} , and experimental isomers shifts S .

System	$S_C(\mu\text{m/s})^{\text{a,b}}$	$S_{\text{SOD}}(\mu\text{m/s})^{\text{a,c}}$	$S(\mu\text{m/s})^{\text{a,d}}$
ZnF ₂	-63.4(3)	+2.4(8.1)	-65.8(8.4)
ZnO (rocksalt)	-20.0(1.1)	+6.7(7.2)	-26.7(8.3)
ZnO (wurtzite)	0.0(1)	0.0(8.2)	0.0(8.3)
ZnS	+54.2(1)	+21.9(8.2)	+32.3(8.3)
ZnSe	+63.7(1)	+20.6(8.2)	+43.1(8.3)
ZnTe	+80.0(1)	+29.6(8.2)	+50.4(8.3)

^a S_C , S_{SOD} , and S are given with respect to a ⁶⁷GaZnO source.

^bReferences 5, 7–10.

^cReference 5.

^d $S = S_C - S_{\text{SOD}}$.

agreement with a previous experimental value³³ of $+(17.4 \pm 3.9) \times 10^{-3} \text{ fm}^2$ (within the error range of the latter) from measurements of ⁶⁵Zn electron-capture decay constants in different chemical environments of Zn metal and ZnO (wurtzite) and then correlating these to the observed ⁶⁷Zn isomer shift in the same systems. We want to stress, however, that in Ref. 33, as in all other previous publications concerning S_{SOD} for ⁶⁷Zn, the isomer shift between Zn metal and ZnO (wurtzite) was derived from the measured center shift, applying again the Debye model to determine S_{SOD} . As mentioned before, the Debye model may be insufficient in this respect. Our present investigation includes a substantial improvement⁵ in the calculation of S_{SOD} with the help of more elaborate lattice-dynamic models, which allow us to take into account both the eigenvalues and eigenvectors of the dynamic matrix. The new value for $\Delta\langle r^2 \rangle$ can, therefore, be considered as more reliable. Furthermore, the good linear correlation between the charge densities and the isomer shifts strongly support the high accuracy of our derived density differences over the series of compounds investigated. Finally, this high degree of linearity suggests that the choice of clusters with external point

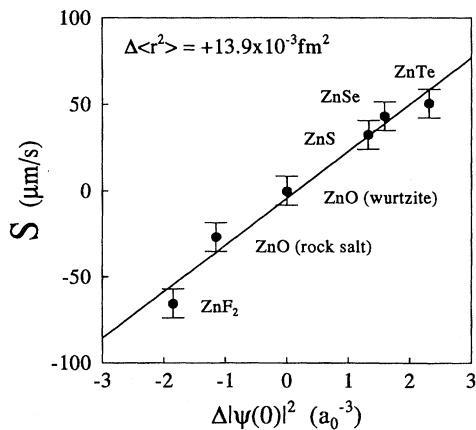


FIG. 6. Calculated results for $\Delta|\psi(0)|^2$ plotted against the experimental isomer shifts. Both sets of data are given with respect to ZnO (wurtzite). For $\Delta|\psi(0)|^2$, the average of the two columns given in Table VI is used, while the experimental isomer shifts are listed in Table VII.

charges for simulating the rest of the infinite lattice represents a good model for calculating the small charge density differences involved.

Before concluding this discussion about $\Delta\langle r^2 \rangle$ for ⁶⁷Zn we would like to compare our results with those of earlier calculations by other methods. A previous evaluation of $\Delta\langle r^2 \rangle$ for ⁶⁷Zn was based⁷ on the concept of isoelectronic pairs between Zn(II) and Sn(IV) compounds. In this method Eq. (2) is used to derive for a pair of isoelectronic compounds,

$$\frac{\Delta\langle r^2 \rangle(\text{Zn})}{\Delta\langle r^2 \rangle(\text{Sn})} = \frac{S(\text{Zn})}{S(\text{Sn})} \frac{\beta(\text{Sn})}{\beta(\text{Zn})} \frac{|\psi(0)|^2(\text{Sn})}{|\psi(0)|^2(\text{Zn})}. \quad (5)$$

The ratio of the densities at the Zn and Sn nuclei are taken from atomic calculations.⁷ Using⁵² $\Delta\langle r^2 \rangle(^{119}\text{Sn}) = 5 \times 10^{-3} \text{ fm}^2$, these authors arrived at $\Delta\langle r^2 \rangle(^{67}\text{Zn}) \approx +11 \times 10^{-3} \text{ fm}^2$ but noted that their result should only be considered an order of magnitude estimate since isoelectronic Zn(II) and Sn(IV) pairs of compounds differ in coordination and principal quantum number of the bonding electrons so that taking ratios of the molecular densities to be comparable to those for atomic densities may be difficult to justify from a quantitative point of view. If one uses the more recently calculated⁵³ value of $\Delta\langle r^2 \rangle(^{119}\text{Sn}) = (6.6 \pm 0.6) \times 10^{-3} \text{ fm}^2$, Eq. (5) gives $\Delta\langle r^2 \rangle(^{67}\text{Zn}) \approx +14 \times 10^{-3} \text{ fm}^2$ which is surprisingly, and perhaps fortuitously, due to the assumptions involved in using Eq. (5), in good agreement with the present result.

A later investigation⁵⁴ of $\Delta\langle r^2 \rangle$ involved a calculation of $|\psi(0)|^2$ for the sphalerite structure zinc chalcogenides ZnO, ZnS, ZnSe, and ZnTe by the scalar relativistic linear muffin-tin orbital (LMTO)⁵⁵ band-structure method in the atomic sphere approximation using the local-density approximation for the exchange and correlation energies. Further, the Zn cores as well as the Zn(3d) orbitals were treated in the frozen-core approximation. It is known⁴⁷ that the Zn(3d) band is located in the gap between the anion valence(s)-like and valence(p)-like orbitals which may introduce additional uncertainty in the results from the investigation in Ref. 54 due to the likely neglect of Zn(3d)-ligand(p) mixing. In the systems studied by these authors, this latter effect would be most important for ZnO (wurtzite). However, this may not be too important since our results indicate that the molecular orbitals associated with Zn(4s) involve no mixing with Zn(3d) for the sphalerite structure compounds. The calculated density differences derived in the present work with respect to the charge density for ZnO (wurtzite) are compared to the LMTO results in Table VIII. Finally, charge densities at the Zn nucleus have also been calculated⁵⁶ for ZnO (wurtzite) and ZnF₂, employing the nonrelativistic multiple scattering (MS-X α) cluster method with the results also summarized in Table VIII. Both the LMTO and MS-X α methods rely on the muffin-tin potential for which the muffin-tin radii are needed as input parameters which may introduce additional uncertainties in those calculations. We are unaware of any calculations other than our own for $\rho(0)$ in ZnO (rocksalt). From Table VIII the agreement between the HF cluster results and the LMTO and MS-X α

TABLE VIII. Comparison of the Hartree-Fock cluster results obtained here, with those from LMTO and MS-X α calculations for $\Delta|\Psi(0)|^2$ (unit: a_0^{-3}).

System	HF Cluster ^a	LMTO ^b	MS-X α ^c
ZnF ₂	-1.9(2)	...	-2.1
ZnO (rocksalt)	-1.1(2)
ZnO (wurtzite)	0.0	0.0	0.0
ZnS	1.3(2)	1.3(2)	...
ZnSe	1.6(2)	1.8(2)	...
ZnTe	2.3(2)	2.4(2)	...

^aThis work.

^bReference 54.

^cReference 56.

calculations is quite reasonable for the various systems where the latter investigations have been carried out. This overall agreement is particularly significant considering the differences in the methods involved and adds to the confidence in the reliability of the Hartree-Fock cluster technique for calculating accurate charge-density differences.

The results of our work differ, however, from the LMTO results in one important respect. The LMTO results were based on the frozen-core approximation and, therefore, the total $\Delta\rho(0)$ for the LMTO is attributed to only the Zn(4s) electrons. Our calculations which include all of the electrons self-consistently show that there is also a sizable contribution to $\Delta\rho(0)$ from the shallow core Zn(3s) electrons. The use of the approximation of a spherical muffin-tin potential for the LMTO and MS-X α is probably not an important source of error for the calculation of $\rho(0)$ calculations because $\rho(0)$ involves *s* density, which is a spherical property.

IV. CONCLUSIONS

The Hartree-Fock cluster procedure has been employed to derive electron densities at the zinc nucleus in the series of compounds ZnF₂, ZnO (rocksalt), ZnO (wurtzite), ZnS, ZnSe, and ZnTe in order to understand the origin of the observed ^{67}Zn Mössbauer isomer shifts. One conclusion from this study is that the Hartree-Fock cluster procedure can be used to calculate accurately very small differences in charge density at the zinc nucleus in systems ranging from nearly ionic to broadband semiconducting compounds involving systems which differ in coordination or ligand. The derived density differences show a very good linear correlation with the isomer shifts. The observed isomer shifts and calculated results for densities at the zinc nucleus have been combined to calculate a value for the nuclear parameter $\Delta\langle r^2 \rangle$, the

difference in mean-square nuclear charge radii between the excited (Mössbauer) and ground nuclear states for ^{67}Zn of $+13.9 \times 10^{-3} \text{ fm}^2$ with an estimated uncertainty of 10%. The present result for $\Delta\langle r^2 \rangle$ agrees with the empirical value of $+(17.8 \pm 3.9) \times 10^{-3} \text{ fm}^2$ within the error bar of the latter. However, considering that the confidence limit in the present work is about a third of the empirically derived result,³³ the value of $\Delta\langle r^2 \rangle$ of $+(13.9 \pm 1.4) \times 10^{-3} \text{ fm}^2$ should be considered more reliable. The most important contribution to $\Delta\rho(0)$ comes from the Zn(4s) electrons with a smaller but significant contribution from the Zn(3s) electrons appearing to arise primarily from the repulsive influence of the ligand-ion orbitals. The Zn(1s) and Zn(2s) contributions to $\Delta\rho(0)$ are comparatively small, opposite in sign, and nearly cancel each other. The dominance of the contribution from Zn(4s) molecular orbitals to $\Delta\rho(0)$ clearly indicates the importance of the covalency in the Zn-ligand chemical bond for the origin of the isomer shifts in these systems in accord with the experimental trend of decreasing isomer shift with increasing ligand electronegativity.

The electronic structures associated with the valence electrons and their approximate atomic-orbital characters show that two different molecular orbitals are primarily responsible for the valence contributions to $\Delta\rho(0)$ in these clusters. The most important of these is the lowest-energy ligand(*p*) orbital in the upper valence band. This molecular orbital has strong covalent mixing of primarily Zn(4s) and ligand(*p*) atomic characters. The second important valence molecular orbital for $\Delta\rho(0)$ has primarily Zn(4s) and ligand(*s*) atomic characters. The general trend for the zinc chalcogenides is that as one goes toward decreasing ionicity of the Zn-ligand chemical bond, the approximate percent Zn(4s) atomic character increases, while the valence ligand(*p*) atomic character decreases, in agreement with the general idea that the covalency of the chemical bond increases in going from ZnO to ZnTe. In addition to these general trends, in the case of ZnF₂, there is significant mixing of Zn(3d) atomic orbitals in the valence orbitals responsible for $\Delta\rho(0)$.

ACKNOWLEDGMENTS

We would like to gratefully acknowledge the continuous support and the excellent cooperation of the cyclotron group at the Kernforschungszentrum Karlsruhe, and would like to thank especially Dr. H. Schweickert, K. Assmus, and W. Maier. This work has been funded by the German Federal Minister for Research and Technology [Bundesminister für Forschung und Technologie(BMFT)] under Contract No. KA2TUM and the Kernforschungszentrum Karlsruhe.

¹R. V. Pound and G. A. Rebka, Jr., Phys. Rev. Lett. **4**, 397 (1960).

²H. deWaard and G. J. Perlow, Phys. Rev. Lett. **24**, 566 (1970).

³G. J. Perlow, W. Potzel, R. M. Kash, and H. deWaard, J. Phys. (Paris) Colloq. **35**, C6-197 (1974).

⁴W. Potzel, Hyperfine Interact. **40**, 171 (1988).

⁵W. Potzel, in *Mössbauer Spectroscopy Applied to Magnetism and Materials Science*, edited by F. J. Long and F. Grandjean (Plenum, New York, 1993), Vol. 1.

⁶D. Griesinger, R. V. Pound, and W. Vetterling, Phys. Rev. B

- 15, 3291 (1977).
- ⁷A. Forster, W. Potzel, and G. M. Kalvius, *Z. Phys. B* **37**, 209 (1980).
- ⁸C. Schäfer, W. Potzel, W. Adlassnig, P. Pöttig, E. Ikonen, and G. M. Kalvius, *Phys. Rev. B* **37**, 7247 (1988).
- ⁹M. Steiner, W. Potzel, C. Schäfer, W. Adlassnig, M. Peter, H. Karzel, and G. M. Kalvius, *Phys. Rev. B* **41**, 1750 (1990).
- ¹⁰H. Karzel, W. Potzel, C. Schäfer, M. Steiner, J. Moser, W. Schiessl, M. Peter, G. M. Kalvius, D. W. Mitchell, S. B. Sulaiman, N. Sahoo, and T. P. Das, *Hyperfine Interact.* **68**, 1067 (1992).
- ¹¹W. Adlassnig, W. Potzel, J. Moser, W. Schiessl, U. Potzel, C. Schäfer, M. Steiner, H. Karzel, M. Peter, and G. M. Kalvius, *Phys. Rev. B* **40**, 7469 (1989).
- ¹²W. Potzel, W. Adlassnig, U. Närger, Th. Obenhuber, K. Riski, and G. M. Kalvius, *Phys. Rev. B* **30**, 4980 (1984).
- ¹³W. Potzel, C. Schäfer, M. Steiner, H. Karzel, W. Schiessl, M. Peter, G. M. Kalvius, T. Katila, E. Ikonen, P. Helistö, J. Hietaniemi, and K. Riski, *Hyperfine Interact.* **72**, 214 (1992).
- ¹⁴A. B. Kunz and D. L. Klein, *Phys. Rev. B* **17**, 4614 (1978).
- ¹⁵K. J. Duff, *Phys. Rev. B* **9**, 66 (1974); W. C. Niewpoort, D. Post, and P. Th. van Duijnen, *ibid.* **17**, 91 (1978).
- ¹⁶K. A. Colbourn and J. Hendrick, in *Computer Simulation of Solids*, edited by C. R. A. Catlow and W. C. Mackrodt (Springer-Verlag, New York, 1982), p. 67.
- ¹⁷J. Sauer, *Chem. Rev.* **89**, 199 (1989).
- ¹⁸N. W. Winter, R. M. Pitzer, and D. K. Temple, *J. Chem. Phys.* **87**, 2945 (1987).
- ¹⁹P. C. Kelires and T. P. Das, *Hyperfine Interact.* **34**, 285 (1987).
- ²⁰H. H. Klauss, N. Sahoo, P. C. Kelires, T. P. Das, W. Potzel, G. M. Kalvius, M. Frank, and W. Kreische, *Hyperfine Interact.* **60**, 853 (1990).
- ²¹D. W. Mitchell, S. B. Sulaiman, N. Sahoo, T. P. Das, W. Potzel, and G. M. Kalvius, *Phys. Rev. B* **44**, 6728 (1991).
- ²²S. B. Sulaiman, N. Sahoo, T. P. Das, O. Donzelli, E. Torikai, and K. Nagamine, *Phys. Rev. B* **44**, 7028 (1991).
- ²³W. H. Bauer and A. A. Khan, *Acta Crystallogr. Sec. B* **27**, 2133 (1971).
- ²⁴C. H. Bates, W. B. White, and R. Roy, *Science* **137**, 993 (1962).
- ²⁵S. C. Abrahams and J. L. Bernstein, *Acta Crystallogr. Sec. B* **25**, 1233 (1969).
- ²⁶R. W. G. Wyckoff, *Crystal Structures I*, 2nd ed. (Wiley, New York, 1965).
- ²⁷L. G. Berry and B. Mason, *Mineralogy* (Freeman, San Francisco, 1959), p. 308.
- ²⁸*Mössbauer Isomer Shifts*, edited by G. K. Shenoy and F. E. Wagner (North-Holland, Amsterdam, 1978).
- ²⁹T. P. Das and E. L. Hahn, *Nuclear Quadrupole Resonance Spectroscopy* (Academic, New York, 1957); M. H. Cohen and F. Reif, in *Solid State Physics*, edited by F. Seitz and D. Turnbull (Academic, New York, 1957), Vol. 5, p. 322.
- ³⁰B. D. Dunlap and G. M. Kalvius, in *Mössbauer Isomer Shifts*, edited by G. K. Shenoy and F. E. Wagner (North-Holland, Amsterdam, 1978), Chap. 2.
- ³¹G. K. Shenoy and B. D. Dunlap, in *Mössbauer Isomer Shifts*, edited by G. K. Shenoy and F. E. Wagner (North-Holland, Amsterdam, 1978), Appendix IV.
- ³²D. A. Shirley, *Rev. Mod. Phys.* **36**, 339 (1964).
- ³³F. Buheitel, W. Potzel, and D. C. Aumann, *Hyperfine Interact.* **47**, 606 (1989).
- ³⁴C. C. J. Roothaan, *Rev. Mod. Phys.* **23**, 69 (1951).
- ³⁵T. H. Dunning and P. J. Hay, in *Modern Theoretical Chemistry*, edited by H. F. Schaefer (Plenum, New York, 1977), Vol. 3, Chap. 1.
- ³⁶*Gaussian Basis Sets for Molecular Calculations*, edited by S. Huzinaga, J. Andzelm, M. Klobukowski, E. Radzio-Andzelm, Y. Sakai, and H. Tatewaki (Elsevier, Amsterdam, 1984).
- ³⁷A. Hinchliffe, *Ab Initio Determination of Molecular Properties* (Hilger, Bristol, 1987).
- ³⁸A. J. H. Wachters, *J. Chem. Phys.* **52**, 1033 (1970).
- ³⁹D. R. Yarkony and H. F. Schaefer, *Chem. Phys. Lett.* **15**, 514 (1972).
- ⁴⁰I. M. Band and V. I. Fomichev, *At. Data Nucl. Data Tables* **23**, 296 (1979).
- ⁴¹R. S. Mulliken, *J. Chem. Phys.* **23**, 1833 (1955); **23**, 1841 (1955).
- ⁴²K. Kunc and H. Bilz, *Solid State Commun.* **19**, 1027 (1976).
- ⁴³K. Thoma, B. Dorner, G. Duesing, and W. Wegener, *Solid State Commun.* **15**, 1111 (1974).
- ⁴⁴C. Benoit and J. Giordano, *J. Phys. C* **21**, 5209 (1988).
- ⁴⁵D. E. Williams and J. Yan, *Adv. At. Mol. Phys.* **23**, 87 (1988).
- ⁴⁶R. Ingalls, F. Van der Woude, and G. A. Sawatzky, in *Mössbauer Isomer Shifts*, edited by G. K. Shenoy and F. E. Wagner (North-Holland, Amsterdam, 1978), Chap. 7.
- ⁴⁷L. Ley, R. A. Pollak, F. R. McFeely, S. P. Kowalczyk, and D. A. Shirley, *Phys. Rev. B* **9**, 600 (1974).
- ⁴⁸C. C. Lu, T. A. Carlson, F. B. Malik, T. C. Tucker, and C. W. Nestor, *At. Data Nucl. Data Tables* **3**, 1 (1971).
- ⁴⁹S. N. Ray, T. Lee, and T. P. Das, *Phys. Rev. B* **8**, 529 (1973).
- ⁵⁰E. Bominaar, J. Guillin, V. R. Marathe, A. Sawaryn, and A. X. Trautwein, *Hyperfine Interact.* **40**, 111 (1988).
- ⁵¹J. A. Majewski and P. Vogl, *Phys. Rev. Lett.* **57**, 1366 (1986); *Phys. Rev. B* **35**, 9666 (1987).
- ⁵²P. A. Flinn, in *Mössbauer Isomer Shifts*, edited by G. K. Shenoy and F. E. Wagner (North-Holland, Amsterdam, 1978), Chap. 9a.
- ⁵³J. Terra and D. Guenzburger, *J. Phys. Condens. Matter* **3**, 6763 (1991).
- ⁵⁴A. Svane and E. Antoncik, *Phys. Rev. B* **33**, 7462 (1986).
- ⁵⁵H. L. Skriver, *The LMTO Method* (Springer, Berlin, 1984).
- ⁵⁶S. Nagel (private communication).